Poly(vinylidene fluoride)/poly(vinyl acetate) miscible blends: 1. Thermal analysis and spectroscopic (*FT*i.r.) characterization

R. E. Belke and I. Cabasso*

The Polymer Research Institute, State University of New York, College of Environmental Science and Forestry, Syracuse, NY 13210, USA

(Received 20 July 1987; revised 22 January 1988; accepted 3 February 1988)

Properties of poly(vinylidene fluoride)/poly(vinyl acetate) miscible blends have been extensively studied using differential scanning calorimetry and Fourier transform infra-red techniques. The thermal analysis revealed that crystallization of poly(vinylidene fluoride) (PVF_2) can be impeded to a large degree by fast cooling from the melt of polyblends containing less than 55 wt% PVF_2. However, after long-term annealing below T_m, or when the blend composition was allowed to cool slowly from the melt, the ratio between amorphous and crystalline PVF_2 blend fractions was almost the same as in the pure polymer. For the components used in this study, this ratio is close to unity. The glass transition (T_g) of this blend is proportionally inverse to the amorphous PVF_2 fraction. The T_g value seems to be progressively influenced by the increase in the degree of crystallinity in the blend, resulting in higher values than those predicted from that extrapolated for the wholly amorphous blend. The latter infers a T_g of less than $-30°C$ for pure PVF_2. Infra-red spectroscopic studies revealed distinct shifts in the symmetrical C–C stretching and skeletal CF–CH–CF bending vibrational bands. Comparison with the reported data for PVF_2/PMMA (poly(methyl methacrylate)) reveals striking similarities, which suggest that the mode of interaction of the ester carbonyl group with the fluorine–carbon–fluorine moiety is equivalent in both blend systems.

(Keywords: poly(vinylidene fluoride); poly(vinyl acetate); blends)

INTRODUCTION

The miscibility of poly(vinylidene fluoride) (PVF_2) and poly(vinyl acetate) (PVAc) has been previously reported[1-5]. Differential thermal analysis (d.t.a.) and dynamic mechanical analysis (d.m.a.) were employed to determine glass transition temperature, crystalline melting temperature and mechanical behaviour as a function of blend composition. Extensive work on this particular blend system was reported by Bernstein *et al.*[1], who showed that PVF_2/PVAc blends can be either completely amorphous or semicrystalline through detailed d.t.a. and d.m.a. measurements. The formation of the PVF_2 crystalline phase was shown to be dependent on the thermal history and blend composition[1-3]. At low concentrations (<30 wt%), PVF_2 is present as an amorphous component in the blend. Long-term annealing above the crystalline melting point of the PVF_2 results in enhanced crystallinity. Paul *et al.*[2] could not detect a cloud point in a ternary solution of PVF_2, PVAc and a common solvent below 350°C. This finding was interpreted as being indicative of a high degree of interaction between the two polymers.

Paul *et al.*[2] dealt with the implications of the melting point depression of PVF_2 in the blend and were able to determine Flory's interaction parameter for a number of PVF_2-containing blends. These interaction parameters were correlated with the corresponding lower critical solution temperatures (*LCST*). Although *LCST* in the PVF_2/PVAc blend system could not be determined, it was assumed that the phase boundary is above the degradation temperature of these polymers.

In comparison to the relatively few reported studies on PVF_2/PVAc blends, a large body of work has been reported on the related PVF_2 and poly(methyl methacrylate) (PMMA) polymer pair[6-16]. The interaction in both blend systems involves an ester carbonyl dipole. The corresponding PMMA blend has been rigorously characterized using infra-red spectroscopic techniques. Coleman *et al.*[14] investigated the PVF_2/PMMA blend system using Fourier transform infra-red spectroscopy (*FT*i.r.). Specific interactions were identified through the use of spectral subtraction. Roerdink and Challa[15] conducted an *FT*i.r. study of PVF_2 blends containing stereoregular PMMA. They determined that the interaction between PMMA and PVF_2 was greater with isotactic as compared to syndiotactic PMMA. In another *FT*i.r. study, Leonard *et al.*[16] demonstrated that a thermally treated PVF_2/PMMA (70:30 wt ratio) blend contains a significant portion of β-PVF_2 crystallites.

In this article we wish to report on further thermal analysis characterization conducted with PVF_2/PVAc blends. The results are compared to those previously reported and serve as a basis for subsequent infra-red spectroscopic characterization. The *FT*i.r. analysis of PVF_2/PVAc blends is reported here, to our knowledge, for the first time. The results reveal significant evidence of interaction in blend specimens containing only amorphous material. These results are also compared with those reported for PVF_2/PMMA blends.

* To whom correspondence should be addressed.

0032-3861/88/101831-12$03.00

Subsequent manuscripts will discuss the effect of PVAc hydrolysis on blend miscibility, of which preliminary results were reported[4,5].

EXPERIMENTAL

Materials

The polymers used in this study were obtained from Polysciences Inc., Warrington, PA, USA, as specified below:

PVF_2, M_n= 60000, Cat. no. 15190 (Lot no. 23843)

PVAc, M_n=500000, Cat. no. 2025 (Lot no. 0106-066)

The solvent used in this work was technical grade *N,N*-dimethyl formamide (DMF), which was distilled before use and further dehydrated on a molecular sieve.

Preparation of blends

Both PVF_2 and PVAc were dissolved in DMF; the solution was cast to yield films that were extensively annealed near the melting temperature of PVF_2. The samples were subjected to an extended drying period in a vacuum chamber prior to analysis. Complete solvent removal was confirmed by infra-red (*FT*i.r.) spectroscopic inspection.

Samples were prepared according to the following procedure: Separate solutions of PVF_2 and PVAc in DMF (10%w/v) were prepared and subsequently mixed in incremental proportions resulting in a series of transparent solutions ranging in PVF_2:PVAc ratios of 9:1 to 1:9 by weight. These solutions were cast on a glass plate in low ambient relative humidity (<20%). The DMF was flashed off at 100°C in an air circulating oven for 30 min followed by a drying period of 60 min at 150°C. The resulting films (10–50 μm) were floated from the glass plates by immersion in cold distilled water followed by drying on 50 μm polytetrafluoroethylene skived carrier tape for 2 h at 90°C. A continually purged nitrogen dry box was used for subsequent film storage.

Characterization methods

Differential scanning calorimetry measurements were conducted with a DuPont 1090B thermal analyser/d.s.c. cell base at a heating rate of 10°C min^{-1}. Sub-ambient cooling was accomplished with a liquid-nitrogen cooling accessory. The cell chamber was continually purged with dry nitrogen at a rate of 20 cm^3 min^{-1}. The d.s.c. cell constant and baseline were verified every 20 runs.

The infra-red spectroscopic studies employed a Nicolet Instruments model 20 DX Fourier transform infra-red spectrometer equipped with a mercury–cadmium–telluride (MCT) cryogenic detector. This study was performed at a wavenumber resolution of 1 cm^{-1}. All spectra shown were the result of an average of 100 scans, and no spectral smoothing was employed. Thin films (10–12 μm) were used to assure spectral subtraction within the range of the Beer–Lambert law. Strongly absorbing peaks, such as those resulting from the ester carbonyl group at 1738 cm^{-1}, are usually a good choice for use as references during the operator-interactive spectral subtraction process since such peaks are assigned to only one component of the polymer pair (i.e. PVAc). However, with thick films (>12 μm) it is not practicable to use this peak as a giude since the absorption at this frequency is too high. In this work the ester carbonyl peak was used in conjunction with several of the other isolated peaks unique to PVAc[5,9] (i.e. 605 and 946 cm^{-1}) to determine the extent of interactive subtraction.

Spectral subtraction techniques were used to assess the infra-red spectra of PVF_2/PVAc blends without the interference of PVF_2 crystalline fraction. Thus, a blend composition of PVF_2/PVAc 20:80 wt ratio that does not contain crystalline moieties was used to identify possible interactive sites in the polymer pair. Subtraction of the PVAc spectrum from that of the blend resulted in the spectrum of amorphous PVF_2. This amorphous PVF_2 spectrum contained peak shifts and broadening not evident in the unblended polymer. The specific peak locations were identified in a subsequent subtraction of pure (semicrystalline) PVF_2 in which non-interactive amorphous absorption peaks were cancelled.

Changing the subtraction order (i.e. subtracting the spectrum of PVF_2 from the PVF_2/PVAc 20:80 wt ratio blend) is somewhat more complicated. In this case a semicrystalline material is subtracted from a binary amorphous blend having no crystallites nor associated interphase. Any resulting information relating to group interaction is obscured by a multitude of extraneaous crystalline and non-interactive spectral data. Interpretation is more difficult when the blend composition is reversed to PVF_2/PVAc 70:30 as discussed in the following text.

RESULTS AND DISCUSSION

Thermal characterization

A compilation of d.s.c. thermograms for PVF_2/PVAc blends is shown in *Figures 1–4*. Data derived from these thermograms are presented in *Tables 1–3*. Second-run scans were chosen for presentation in *Figures 1* and *2* since a known thermal history was established during the previous d.s.c. scan; the cooling rate following the first run was -60°C min^{-1}. The results shown are quite similar to the data reported by Bernstein *et al.*[1], who used differential thermal analysis (d.t.a.) to study the blends. Notable trends included a composition-dependent glass transition temperature and significant depression of the PVF_2 crystalline melting point as the PVAc proportion is increased. *Figure 2* allows a full appreciation of the magnitude of melting point depression in this system. As with the prior d.t.a. study[1], endotherm peaks are used in data interpretation. At the composition of PVF_2/PVAc 30:70 the crystalline melting temperature is 151°C in contrast to 168°C for the pure PVF_2.

Crystallization behaviour. The thermograms of the samples in intermediate compositions, 30–50 wt ratio PVF_2 (traces D–F in *Figure 1*), exhibit a recrystallization exotherm. Almost identical ΔH_f values were recorded for the exotherms and the endotherms in these scans. This indicates that under the quoted rate of cooling from the melt (quenching) there is sufficient PVAc to suppress crystallization for compositions up to 50 wt% PVF_2. In this series, recrystallization exotherms could not be detected for compositions of 60 wt% or more PVF_2, although a crystalline endotherm exists. Two reasons for this characteristic relate to the composition and thermal history of the blend. The glassy state may be reached without crystallization if the rate of cooling is faster than the crystallization rate. This is directly related to the

Table 1 Thermodynamic data for PVF_2/PVAc blends as derived from differential scanning calorimetry (d.s.c.) thermograms in *Figure 1*

Scan	Blend composition, PVF_2 (wt%)	T_g onset (°C)	Heat of fusion[a], ΔH_f ($J\,g^{-1}$)	Melting temperature (°C)
A	0	38.1	–	–
B	10	32.0	–	–
C	20	28.5	–	–
D	30	25.3	2.72	151.3
E	40	28.0	18.8	153.9
F	50	30.1	24.5	156.5
G	60	23.0	29.6	161.1
H	70	18.7	33.2	163.8
I	80	11.0	43.8	163.3
J	100	–	48.5	168.2

[a] ΔH_f based on total sample weight

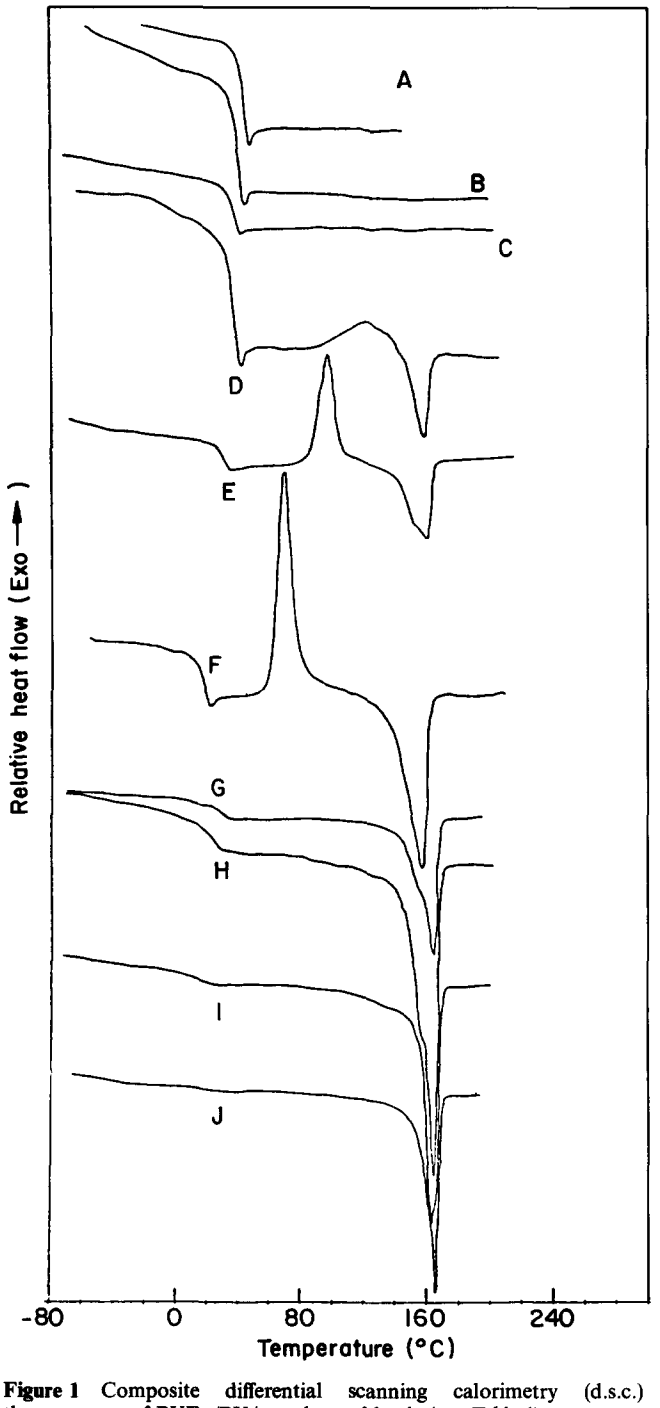

Figure 1 Composite differential scanning calorimetry (d.s.c.) thermograms of PVF_2/PVAc polymer blends (see *Table 1*)

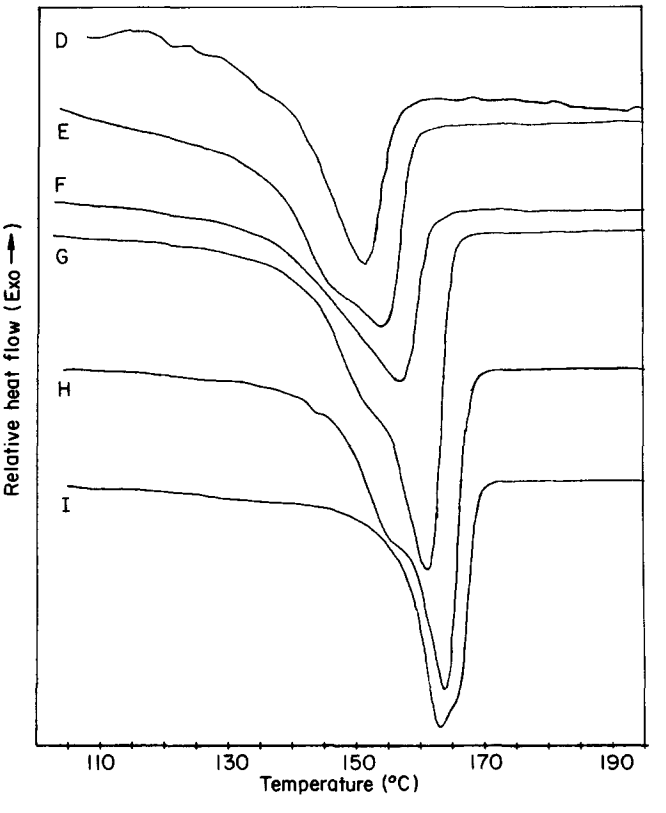

Figure 2 Expanded melting region of selected PVF_2/PVAc polymer blends (scans D–I from *Figure 1*)

location of the crystallization temperature T_c (of the different blend compositions) obtained by cooling from the melt. Thus, samples with progressively higher PVF_2 contents recrystallize at lower temperatures (*Figure 1*, scans D–F) and show progressively higher T_c values (see *Figure 4*).

These findings prompted a detailed study of the blend in the composition range of 50–60 wt% PVF_2. A series of PVF_2:PVAc blends in this composition range were prepared according to the same procedure delineated in the 'Experimental' section. A thermal history was established for each sample by cooling at a rate of 60°C min^{-1} from 200°C. The resulting d.s.c. scans are shown in *Figure 3*. A recrystallization exotherm appears only for the PVF_2/PVAc 50:50 composition. These results are reinforced by the corresponding quenching curves shown in *Figure 4*. In the latter, both the

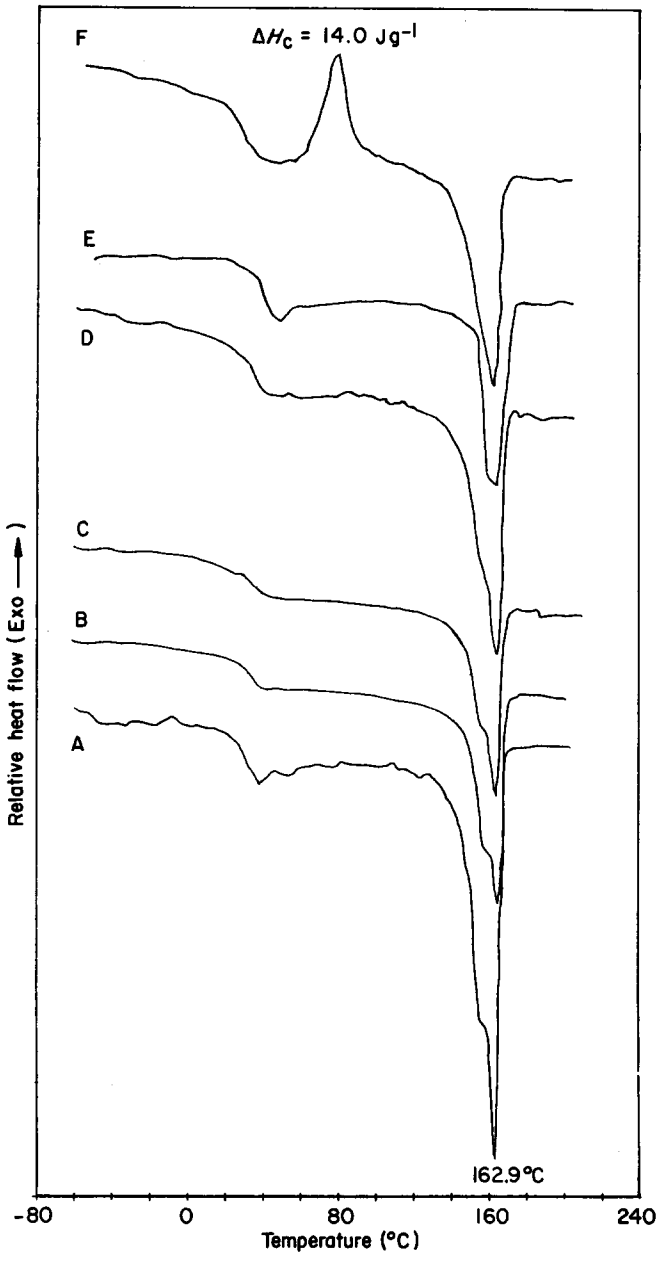

Figure 3 Differential scanning calorimetry (d.s.c.) thermograms of PVF_2/PVAc blends in the compositional range 50–60 wt% PVF_2. Heating rate = 10°C min^{-1} (see *Table 2*)

crystallization temperatures (T_c) and the magnitude of the corresponding exotherms are shown to decrease with decreasing PVF_2 content in the blends. The crystallization kinetic is also sharply affected by the depression of T_c, as evidenced by the progressive broadening of the exotherms. For the 50 wt% PVF_2 composition, the crystallization peak is not shown. However, according to *Figure 3* (and *Table 2*) partial crystallization indeed took place before reaching the glassy state. It is worth noting that the glass transition of this system also increases at the same time owing to the increase of the PVAc fraction. Thus, it appears that the abrupt impediment to crystallization that occurs for compositions below 52 wt% PVF_2 is a result of both rate of cooling and insufficient PVF_2 concentration.

It can be deduced that the crystallization time required for samples B and C (*Figure 1*) is much longer than allowed under the experimental conditions. Indeed, it was

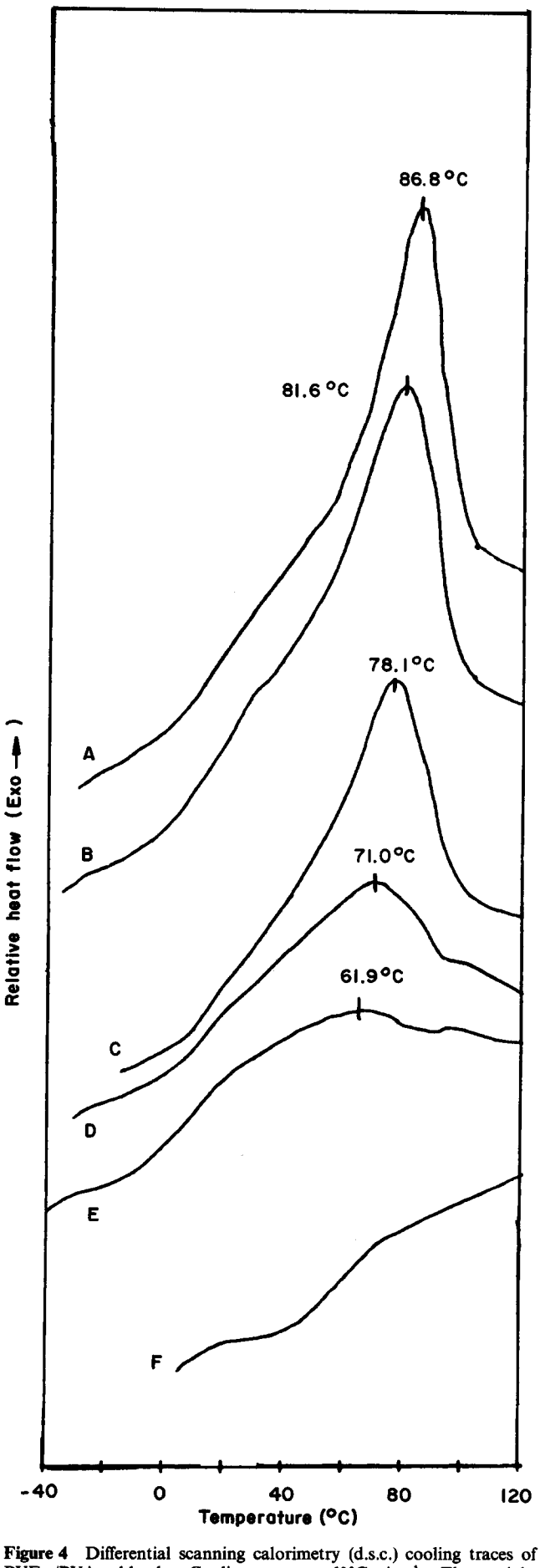

Figure 4 Differential scanning calorimetry (d.s.c.) cooling traces of PVF_2/PVAc blends. Cooling rate = −60°C min^{-1}. The weight fractions (%) of PVF_2 in the samples are: A, 60; B, 58; C, 56; D, 54; E, 52; F, 50

observed that annealing samples B and C for 30 min at 150°C resulted in limited PVF_2 crystallization. This was also shown by Bernstein *et al.*[1], who annealed a similar blend composition for 5 days at 130°C. Correlation between the heat of fusion (ΔH_f) and the composition of the blend is shown in *Figure 5*. This plot indicates that annealed PVF_2/PVAc samples containing less than 20 wt% PVF_2 do not exhibit a crystalline fraction even when subjected to annealing, and therefore may be treated as wholly amorphous blends (a fact that was exploited in the following infra-red characterization of the blend.)

Table 2 Melting temperatures and heats of fusion for six PVF_2/PVAc blends within the compositional range of PVF_2 50–60% (see *Figure 3*)

Scan	PVF_2/PVAc (wt%)	Melting temperature (°C)	Heat of fusion, ΔH_f ($J\,g^{-1}$)
A	60/40	162.9	28.8
B	58/42	162.8	31.5
C	56/44	162.0	27.0
D	54/46	161.4	26.9
E	52/48	160.5	27.9
F	50/50	158.8	23.8

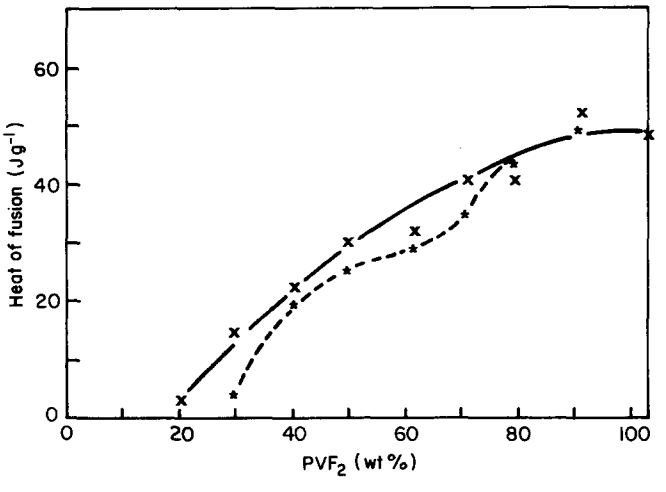

Figure 5 Heat of fusion ($J\,g^{-1}$) as a function of weight percentage of PVF_2 fraction in PVF_2/PVAc blend (see *Table 1*): ×, annealed sample; ∗, second run

The curves in *Figure 5* show that the heat of fusion recorded for the annealed samples are consistently higher than those found after rapid quenching for compositions below 70 wt% PVF_2 (see also *Table 1*). The samples containing more than 70 wt% PVF_2 have apparently had ample time to crystallize fully during the cooling period. Therefore the heat of fusion of annealed and unannealed samples in this compositional range is the same.

The effect of thermal history on the amorphous/crystalline ratio in these compositions is shown in *Figure 6*. This is a plot derived from the d.s.c. data shown in *Table 3* and represents two different thermal histories. The amorphous/crystalline ratio was calculated by normalizing individual blend ΔH_f values to PVF_2 content and using a single-crystal ΔH_f value[17] of 105 $J\,g^{-1}$. In this plot, ACEF delineates the amorphous fraction in PVF_2/PVAc blends produced by cooling from the melt at $-60°C\,min^{-1}$. The corresponding crystalline fraction is

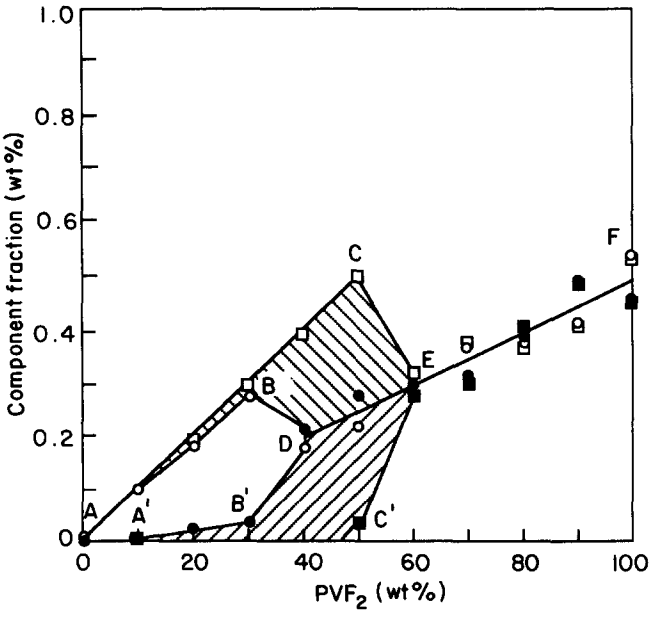

Figure 6 Crystalline or amorphous fraction of PVF_2 vs. fraction of PVF_2 in its blends with PVAc. The cycles ACEC'A and ABDB'A'A represent two different thermal histories: crystalline (■), amorphous (□), in quenched blends; crystalline (●), amorphous (○), in annealed blends

Table 3 Relative fraction of amorphous and crystalline PVF_2 in blends with PVAc having two thermal histories (designated annealed and quenched) as determined by differential scanning calorimetry

Blend PVF_2 content (wt%)	PVF_2 distribution (wt%)			
	Annealed[a]		Quenched[b]	
	Crystalline	Amorphous	Crystalline	Amorphous
0	–	–	–	–
10	0	0.10	0	0.10
20	0.02	0.18	0	0.20
30	0.02	0.28	0	0.30
40	0.22	0.18	0	0.40
50	0.28	0.22	0.01	0.49
60	0.30	0.30	0.28	0.32
70	0.38	0.32	0.32	0.38
80	0.40	0.40	0.42	0.38
90	0.49	0.41	0.45	0.45
100	0.46	0.53	0.46	0.54

[a] Blends were annealed at 150°C for 1 h and then allowed to cool at ambient (23°C)
[b] Blends were heated to 200°C and cooled at $1°C\,s^{-1}$

Table 4 Measured and calculated glass transition temperatures of PVF_2/PVAc blends

Composition, PVF_2 (wt%)	D.s.c. run[a] no.	Observed blend T_g (onset) (°C)	Fraction of amorphous PVF_2				T_g blend[d] (°C)
			Based on total[b]		Based on amorphous[c]		
			(wt%)	(vol%)	(wt%)	(vol%)	
0	1	38.1	–	–	–	–	–
10	1	32.0	10.0	7.3	10.0	7.2	32.8
		32.5	10.0	7.3	10.0	7.2	32.8
20	1	28.0	18.1	13.6	18.5	13.8	28.0
	2	28.5	20.0	15.0	20.0	15.0	27.1
30	1	25.3	27.8	21.6	28.4	21.9	22.1
	2	22.1	30.0	23.3	30.0	23.3	21.1
40	1	28.0	18.1	13.6	23.2	17.6	25.2
	2	21.7	40.0	32.1	40.0	32.1	14.6
50	1	30.1	22.4	17.1	30.9	24.1	20.5
	2	11.8	50.0	41.5	50.0	41.5	7.8
60	1	23.0	30.0	23.3	42.9	34.7	12.7
	2	20.0	31.8	24.8	44.3	36.0	11.8
70	1	18.7	32.0	24.9	51.6	43.0	6.7
	2	14.0	38.3	30.8	56.1	47.5	3.4
80	1	11.0	39.7	32.0	61.5	53.1	−0.7
	2	9.2	38.3	30.8	65.7	55.6	−2.5

[a] 1 = d.s.c. run following slow cooling from anneal at 150°C;
2 = d.s.c. run following −60°C min^{-1} quench from 200°C
[b] PVF_2 (amorph)/(PVF_2 + PVAc) (%)
[c] PVF_2 (amorph)/PVF_2 (amorph) + PVAc) (%)
[d] $T_{g\,blend}$ calculations based on only amorphous material (see equation (1))

outlined in AC'EF. The lines ABDF and AA'B'DF represent the compositions of the same blend samples annealed at 150°C for 60 min and then allowed to cool slowly at ambient to 23°C for 20 min.

Both examples, which are represented by the cycles ABDB'A' and ACEC'A', seem to collapse along the line DEF. This line maintains the ratio of amorphous: crystalline PVF_2 in the blend more or less constant as the fraction of the PVF_2 in the blend increases (see also *Table 3*). It is perhaps a somewhat peculiar observation, unique to the polymer grades used in this study, that this ratio is close to unity. More important is the fact that in spite of the presence of PVAc, which was shown to affect crystalline properties, such as melting point depression, the PVF_2 component in the blend seems split along the line DEF close enough to the ratio that would have been predicted from the pure PVF_2 (which is about 46% crystalline). This suggests that the line DEF represents the composition for which the blends are in equilibrium, at least within the time frame of the experiment (i.e. 3 months). Therefore a large segment of line AC represents a metastable state produced by the fast cooling from the melt. Slower cooling rates, which produced line AB, can be further shortened by extension of the residence time in the interval between T_m and T_g.

Figure 6 raises some interesting questions as to the thermodynamic equilibrium of the PVF_2/PVAc blend. The annealing experiments, reported by Bernstein *et al.*[1] and this work, suggest that the line DEF can be extended further, i.e. to blend compositions of less than 30% PVF_2. Whether or not the ratio between amorphous and crystalline PVF_2 is truly altered in this region or is just a consequence of PVAc impedance of the rate of crystallization has yet to be resolved.

Compositional dependence of T_g. Assessment of the compositional dependence of the glass transition temperature (T_g) in semicrystalline blends is often complex when compared to blends based on wholly amorphous polymers. The crystalline domains are not available for polymer pair interactions, and in this work a plot of the glass transition temperature as a function of the amorphous content of PVF_2 in the blend was drawn (*Figures 7a* and *7b*). This was accomplished by calculating the crystalline fraction of the PVF_2 in the blend composition using the heat of fusion value of a single crystal[18]. The computed crystalline fraction in the blend was then subtracted, and the balance considered to be amorphous PVF_2. This seems to be a more relevant presentation than plotting T_g as a function of total PVF_2 weight fraction (crystalline and amorphous)[1]. In the latter it was implied that, by extrapolation, the T_g of the pure PVF_2 was less than −10°C. The reported glass transition temperature of PVF_2, however, is in the neighbourhood of −35°C[19]. The resolution of the T_g of pure PVF_2 with d.s.c. is difficult and multiple values have been reported[1,9,12,15,20]. A plot of T_g vs. volume percentage (rather than weight percentage) is given in *Figure 7a*. This was necessitated by the significant density disparity between the subject polymers (amorphous PVF_2, 1.68 g cm^{-3} (refs. 19, 28); PVAc, 1.19 g cm^{-3} (ref. 21)). The linear plot would correspond to:

$$T_{g\,blend} = \sum_i \phi_i T_{gi} \qquad (1)$$

where ϕ is the volume fraction[22].

The fit of the data shown in *Figure 7a* to this equation is tenuous at blends of high PVF_2 content, apparently due to the crystalline fraction in the blend. Thus the plot shown in *Figure 7a* indicates that extrapolation to −35°C for pure PVF_2 is not as straightforward as that recently displayed by Wu[23] for PVF_2/PMMA. However, the extrapolation to ca. −35°C (*Figure 7a*) holds for the first 20–25 vol%; as the PVAc fraction in the blend decreases and PVF_2 crystals are formed, deviation from the linear plot for the quenched, and more for the annealed,

becomes apparent. The relationship between T_g and weight percentage of amorphous PVF_2 is also given (*Figure 7b*) for the convenience of the reader.

FTi.r. characterization

Several papers have been previously cited in which spectral subtraction was used to give a clear indication of interaction between PVF_2 and other compatible polymers[14–16]. The same procedure was performed in the course of this investigation for PVF_2/PVAc blends. The two illustrative blend compositions to be discussed in this paper are the PVF_2/PVAc 20:80 and PVF_2/PVAc 70:30 blends. The former is amorphous and the latter is a semicrystalline blend (see also *Tables 5* and *6*).

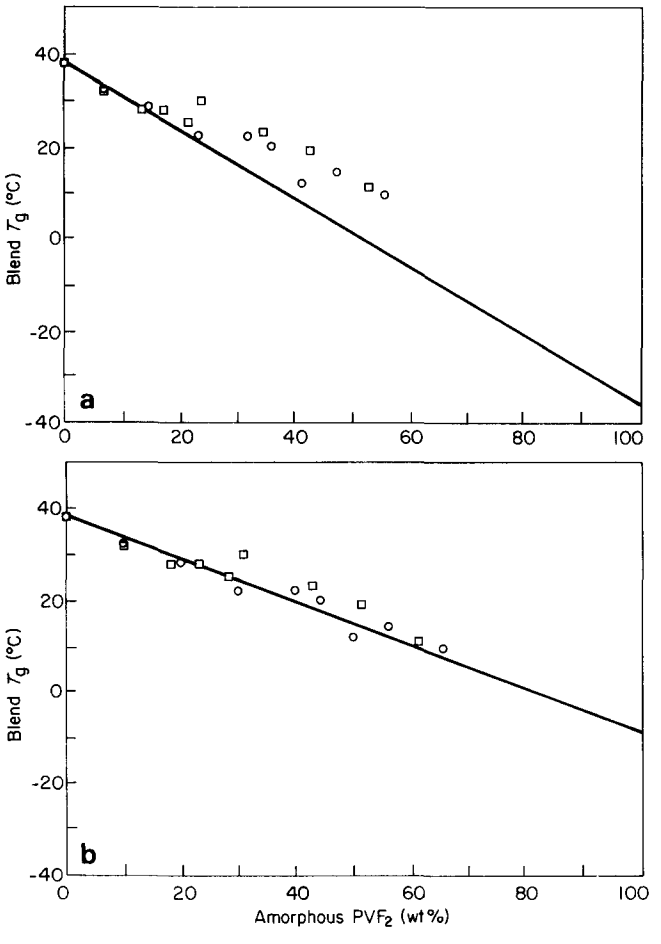

Figure 7 Experimentally determined T_g of PVF_2/PVAc blend vs. (a) amorphous volume fraction of PVF_2 and (b) amorphous weight fraction of PVF_2, (i.e. PVF_2 (amorph)/[PVF_2 (amorph) + PVAc] × 100: ○, from quenched sample; □, from annealed sample

FTi.r. evaluation of the PVF_2/PVAc 20:80 blend. The first blend of interest is an amorphous material (*Figure 1* and *Table 1*) whose composition (PVF_2/PVAc 20:80 wt ratio) is suitable for an infra-red subtraction study since enough PVF_2 is present to lead to unambiguous conclusions. Four *FT*i.r. absorbance spectra in the range 400–2000 cm^{-1} are shown in *Figure 8*. Spectra A and B are composed of pure PVAc (amorphous) and PVF_2/PVAc 20:80, respectively. Subtraction of A from B results in spectrum C. The spectrum labelled D is of pure semicrystalline PVF_2. It is apparent that subtracted spectrum C is different from that of pure PVF_2 (spectrum D).

The oscillation band centred ca. 1738 cm^{-1} in spectra A and B is assigned to the ester carbonyl peak vibrational band, which broadens as indicated by the positive absorption at 1709 cm^{-1} and negative absorption at 1750 cm^{-1}, shown in spectrum C. However, owing to the high absorption of the carbonyl, even a slight broadening of the peak in B compared to A (or inversely) would yield the split shown in C. Other notable band mismatches in

Table 6 Infra-red absorption peak assignments for PVAc

PVAc peaks (cm^{-1})	Peak assignments[27]
2976	asym CH_3 stretch
2924	sym CH_2 stretch
1740 (1738)[a]	C=O stretch
1435	CH_2 scissor
1374	CH_3 wag
1238 (1241)	CO–O stretch
1122 (1123)	C–O–C + C–C–C stretch
1020 (1021)	sym C–C–C stretch
948 (947)	C–CH_3 rock
794 (795)	sym C–CH_3 stretch
605	CH_3–CO_2 stretch

[a] ( ) = observed locations in reported spectra

Table 5 Infra-red absorption peak assignments for PVF_2

PVF_2 peaks (cm^{-1})	Phase assignment	Peak assignments[24]
3024		asym CH_2 stretch
2989		sym CH_2 stretch
1424 (1423)[a]		CH_2 bend − CH_2 wag
1405		CH_2 bend + CH_2 wag − antisym C–C stretch
1384 (1383)	cryst.[16]	CH_2 bend + CH_2 wag
1294		asym CF_2 stretch − CF_2 rock
1212	cryst.[16]	asym CF_2 stretch + CH_2 wag
1183		sym CH_2 stretch + CH_2 twist
1151		asym C–C stretch − CF_2 rock
1070	cryst.[16]	sym C–C stretch
975	cryst.[15,16,18]	CH_2 twist
875	amorph.[14]	sym C–C stretch + skeletal CF–CH–CF bend
855	cryst.[15,16]	CH_2 rock
796	cryst.[15,16,18]	CH_2 rock
763	cryst.[15,16,18]	CF_2 bend + skeletal CF–CH–CF bend
615	cryst.[15]	CF_2 bend − skeletal CH–CF–CH bend
533	cryst.[15,18]	CF_2 bend
489		CF_2 bend + CF_2 wag

[a] ( ) = observed locations in reported spectra

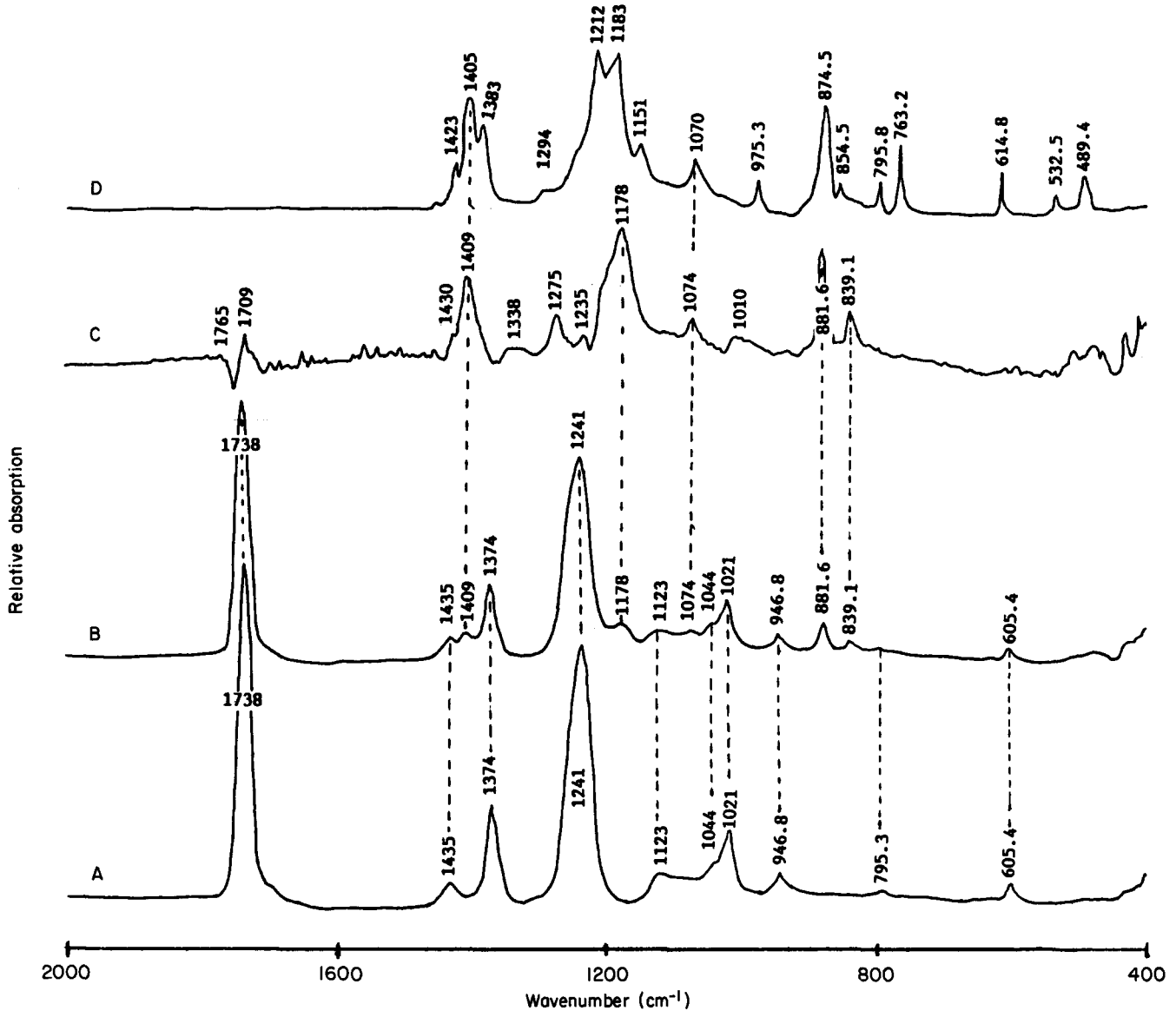

Figure 8 Comparison of four *FT*i.r. absorption spectra; A, pure PVAc; B, PVF_2/PVAc (20:80) blend; C, spectrum B minus spectrum A; D, pure PVF_2 (including α crystalline polymorph)

spectrum B in *Figure 8* were identified at 1409, 1178, 881 and 839 cm^{-1} and were further analysed. These spectral changes suggest interactions between the blend components. It is instructive to note that three of these bands are in the same location found in the corresponding PVF_2/PMMA blend evaluated in a similar manner[15].

The absence of the distinctive PVF_2 absorption peaks at 532, 614, 763, 795, 854, 975, 1183, 1212 and 1383 cm^{-1} in spectrum C in *Figure 8* is notable. However, these findings are in close correspondence with the results obtained by the Roerdink and Challa[15] study involving PVF_2 interaction with stereoregular poly(methyl methacrylate) (PVF_2/PMMA 20:80) and correspond to interactive PVF_2 peaks in the Coleman *et al.* study[14] of PVF_2/PMMA 25:75. Roerdink and Challa[15] used both 80 wt% atactic and isotactic PMMA blended with 20% PVF_2. The mode of dipole – dipole interaction is thought to be the equivalent in the PVF_2/PMMA and PVF_2/PVAc systems, in that both interactions involve ester carbonyl with fluorine–carbon–fluorine structural moieties. The findings presented in *Figure 8* support this hypothesis. The specific lost PVF_2 vibrational bands reported in the Roerdink and Challa study are: 530, 610, 760, 795, 855, 970, 1065, 1182, 1213, 1292 and 1382 cm^{-1}. In all cases, the lost PVF_2 vibrational bands are attributed to crystalline absorptions since all of the aforementioned blend compositions contain only amorphous material. The crystalline origin of this last set of peaks is supported by the work of Cortili and Zerbi[24].

In addition to the absence of the above peaks in the subtraction spectrum, there is evidence of vibrational band shifting when the subtraction spectrum is compared to the pure PVF_2. Distinct shifts are observed in the symmetrical C–C stretching and skeletal CF–CH–CF bending vibrational bands from 874.5 cm^{-1} in the pure material to 881.6 cm^{-1} in the PVF_2/PVAc blend. Such shifts can also be found in the respective infra-red spectra of amorphous PVF_2/PMMA blends[14,15,24].

It is apparent from *Figure 8* that blending of PVF_2 and PVAc gives rise to a new peak centred ca. 1178 cm^{-1}. This strong, broad peak has a definite shoulder to the left that appears to be the remnant of the 1183 cm^{-1} PVF_2 vibrational band. A more definitive manner in which to evaluate this situation is to differentiate between

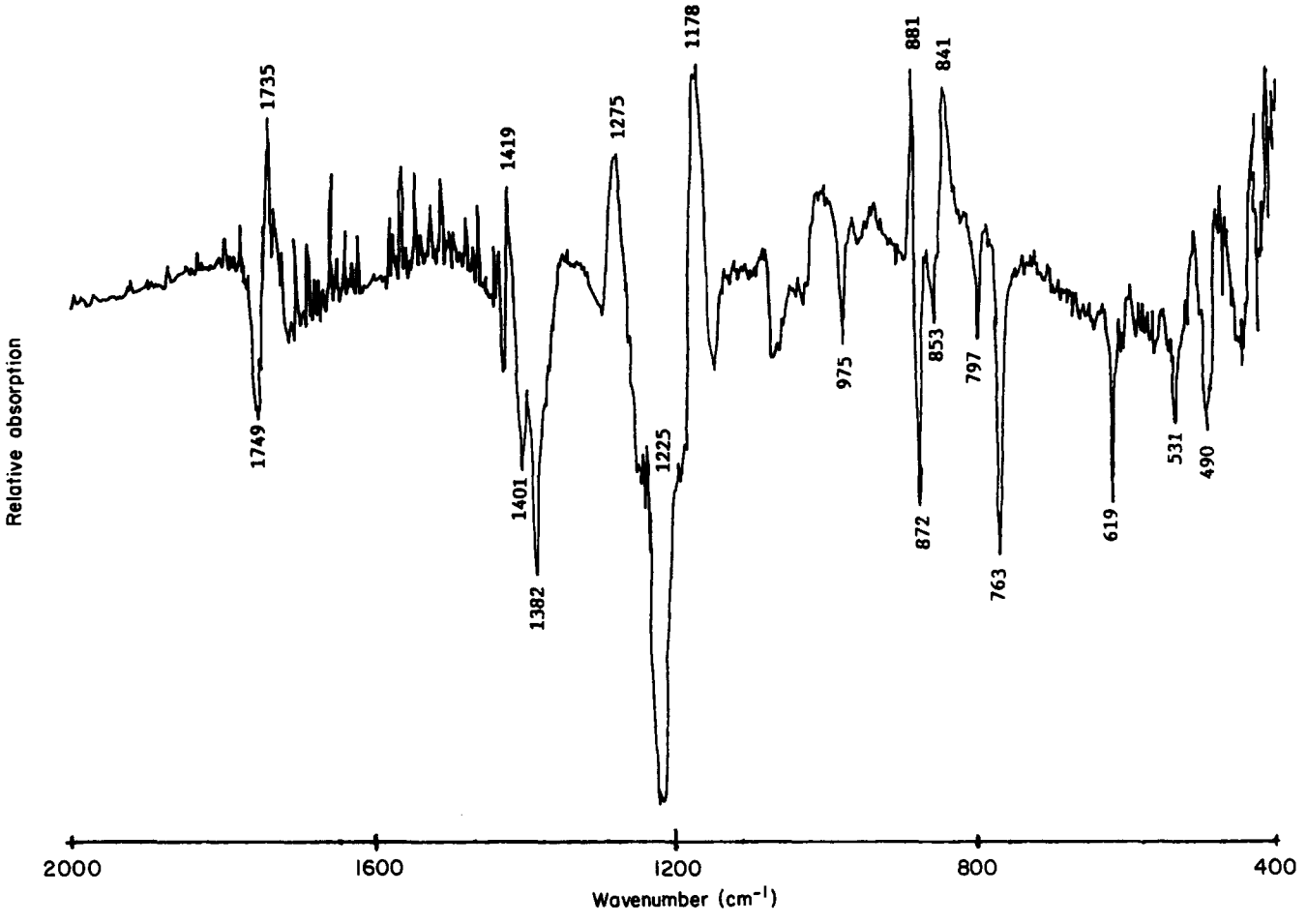

Figure 9 Double subtraction *FTi.r.* spectrum: {[PVF_2/PVAc (20:80)] − 100% PVAc} − 100% PVF_2

interactive and non-interactive amorphous PVF_2 peaks with a second spectral subtraction.

Subtraction of the spectrum of amorphous PVAc from that of the PVF_2/PVAc 80:20 blend, containing only amorphous PVF_2, results in a spectrum derived from only amorphous PVF_2 absorbance (spectrum C in *Figure 8*). This amorphous PVF_2 spectrum contains spectral information from both interactive and non-interactive polymers. These two components may, in turn, be separated through a second process in which the spectrum of semicrystalline PVF_2 is subtracted from the amorphous PVF_2 spectrum. The resulting subtraction spectrum shows upward peaks derived from amorphous interactive absorptions and downward peaks caused by crystalline PVF_2 regions (*Figure 9*). The non-interactive amorphous PVF_2 vibrational bands common to both parent spectra in the last subtraction are cancelled.

These results pinpoint the location of the absorption bands that have either been shifted from their original position in pure semicrystalline PVF_2 or been created due to amorphous interaction. The interactive subtraction procedure also allows discrimination between new peak formation and peak shifting. The apparent new peak in C in *Figure 8* is the result of the shifting of the 1183 cm^{-1} symmetrical CH_2 stretching and twisting band to the 1178 cm^{-1} position. Aside from the ester carbonyl oscillation band, there are five major peaks (*Figure 9*) due to amorphous interaction located at 1419, 1275, 1178, 881 and 841 cm^{-1}. The peaks at 1419 and 881 cm^{-1} are accompanied by strong oscillatory bands, indicating shifting from their original locations at 1424 cm^{-1} (downward shift) and 875 cm^{-1} (upward shift). The 1424 cm^{-1} peak arises from CH_2 movements, while the 875 cm^{-1} peak is assigned to symmetric C–C stretching and skeletal CF–CH–CF bending. This spectrum suggests that not only the carbon–fluorine dipole groups are affected by blending, but the neighbouring CH_2 groups as well.

Figure 10 compares the double subtraction spectra with both the absorption spectra of semicrystalline PVF_2 (spectroscopically identified as the α polymorph) and the first subtraction result. The intensities of the crystalline peaks were adjusted to be identical so that the amorphous interactive peaks were apparent. The resulting effect is to have the common crystalline peaks appear as mirror images of each other in the top two spectra. The most obvious case of broadening involves the peak at 1275 cm^{-1} in the double subtraction (top) spectrum. This is a weak, minor peak in pure PVF_2 and is assigned to CF_2 movements. The double subtraction results show that this peak increases many times in intensity in an amorphous miscible blending situation. These results substantiate the argument that the ester carbonyl and fluorine–carbon–fluorine dipoles are interacting in this blend system.

FTi.r. evaluation of the PVF_2/PVAc 70:30 composition. A similar spectral subtraction study was performed on the blend composed of PVF_2/PVAc 70:30. As is shown in *Figure 1* and *Table 1*, this blend is

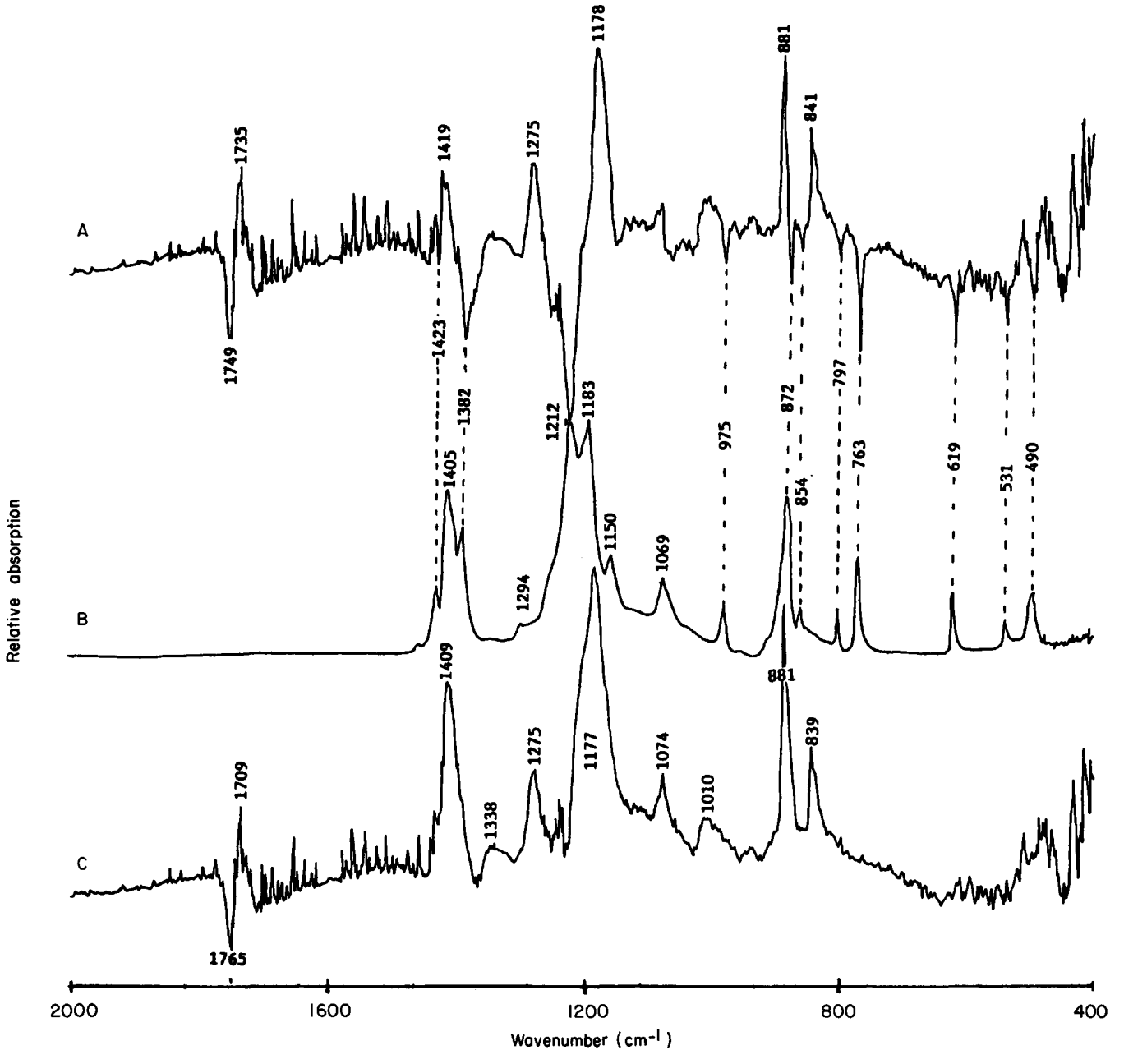

Figure 10 *FT*i.r. absorption spectra of: A, {[PVF_2/PVAc (20:80)] – PVAc} – PVF_2; B, 100% PVF_2 (including α crystalline polymorph); C, [PVF_2/PVAc (20:80)] – PVAc

composed of two phases, i.e. an amorphous blend and a nearly pure crystalline PVF_2. Therefore, it may be viewed as a heterogeneous system. This binary-phase scenario is clouded by the presence of an interphase[17,25].

Figure 11 shows the subtraction spectra (subtracting the PVAc component) of the blends containing 70% PVF_2 (A) and 20% PVF_2 (B) respectively. These are compared to that of pure PVF_2 (C). Spectra A and B do not match due to the semicrystallinity of the former. Note that the ester carbonyl remnant shows little or no evidence of the oscillation band quite evident in the previous subtraction. The remnant of the carbonyl persists since this vibrational band was saturated in the parent blend spectrum. There is a peak-to-peak correspondence between scans C and A, showing that the majority of the peaks belong to the PVF_2 fraction that does not interact with the PVAc. These results are also supported by the work of Roerdink and Challa with the PVF_2/PMMA miscible blend system[15].

The spectroscopic results shown in *Figure 11*, however, indicate substantial interactions in the 70:30 blend. The crystalline fraction yields a more complex spectrum than found with the corresponding 20:80 blend. The subtraction of PVAc (*Figure 11*, scan A) and subsequent subtraction of the PVF_2 (*Figure 11*, scan C) was expected to point out vibrational bands involved in amorphous interaction. However, the results of this subtraction, shown in *Figure 12*, are not as conclusive. When the spectrum of the semicrystalline PVF_2 (*Figure 11*, scan C) is subtracted from that shown in A, a choice may be made to cancel either the crystalline or non-interactive amorphous material, but not both. This complicates the result (*Figure 12*), which is 'contaminated' by the component that was not cancelled, and its spectral

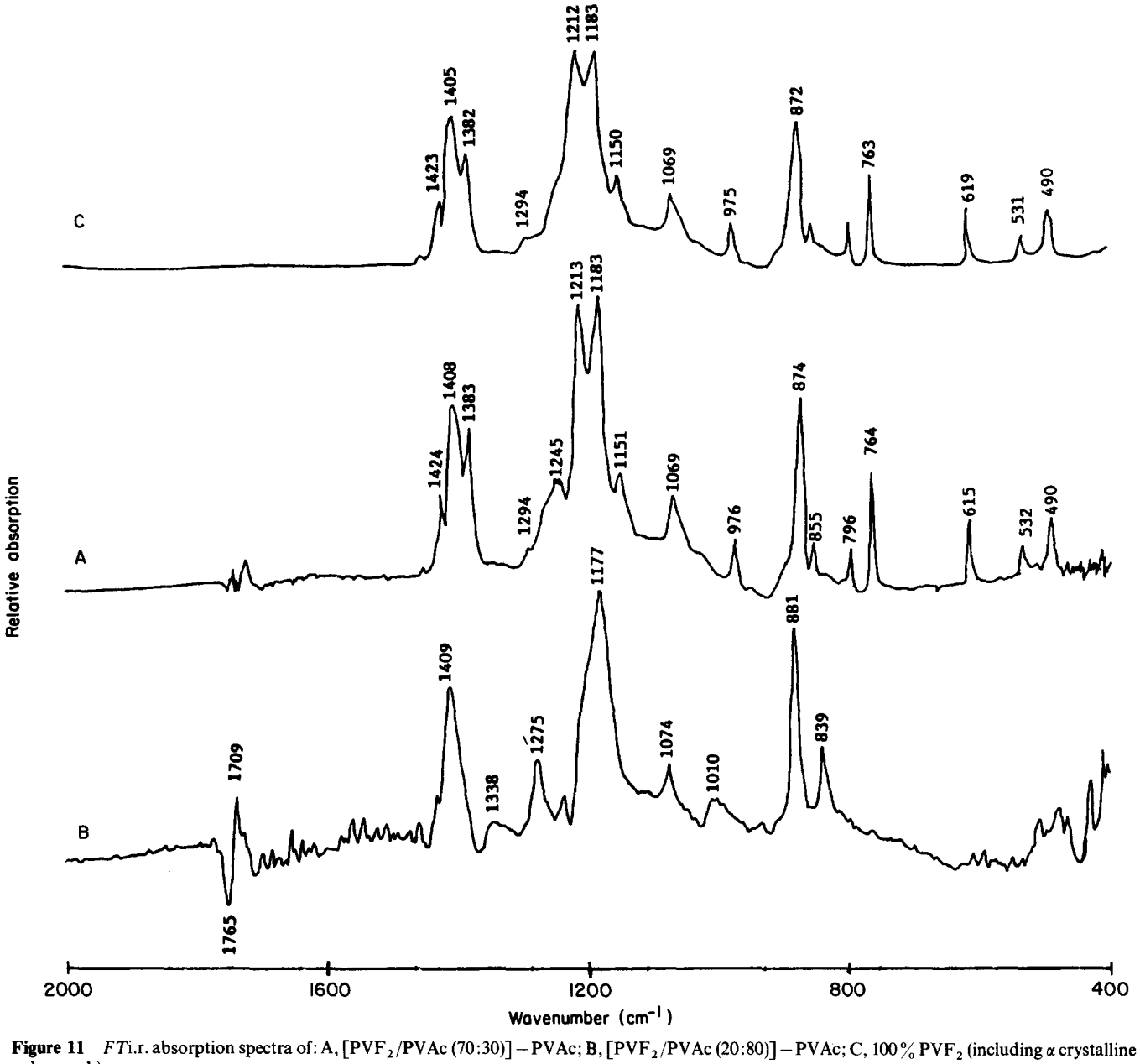

Figure 11 *FT*i.r. absorption spectra of: A, $[PVF_2/PVAc\ (70:30)] - PVAc$; B, $[PVF_2/PVAc\ (20:80)] - PVAc$; C, 100% PVF_2 (including α crystalline polymorph)

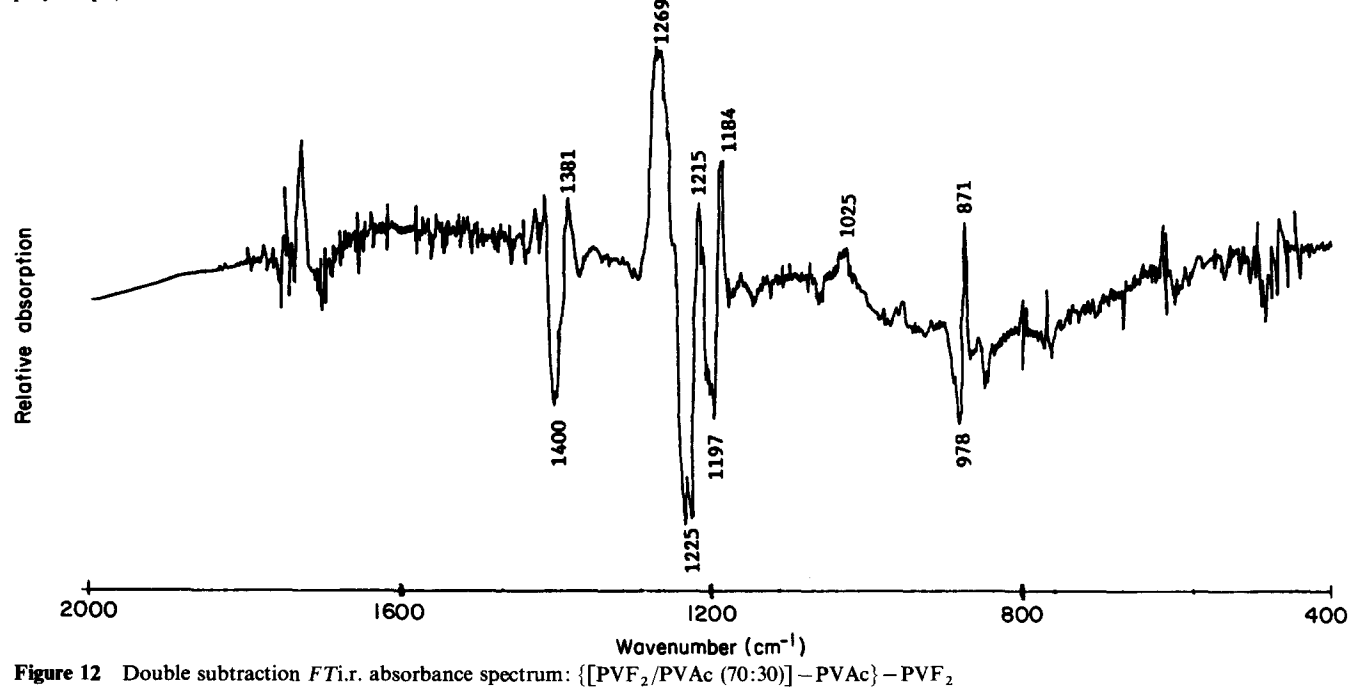

Figure 12 Double subtraction *FT*i.r. absorbance spectrum: $\{[PVF_2/PVAc\ (70:30)] - PVAc\} - PVF_2$

contribution therefore clouds interpretation. In summary, the subtraction results in *Figure 12* are different from the corresponding PVF_2/PVAc 20:80 double subtraction spectrum (*Figure 9*).

CONCLUSIONS

The purpose of this work was to shed some light on the characteristics of the miscible semicrystalline PVF_2/PVAc blend system through detailed d.s.c. and *FT*i.r. analysis. The d.s.c. portion of this investigation compares well with previously reported thermal analysis studies. There is no doubt that PVAc interferes with the crystallization mode of PVF_2. However, there seems to be an ultimate tendency for the PVF_2 to form a nearly constant amorphous/crystalline ratio. There is a strong indication that this tendency can be extended to blends with lower concentration than 30 wt% PVF_2. The glass transition of this blend is proportionally inverse to the amorphous PVF_2 fraction. Individual T_g values seem to be progressively influenced by the increase in the degree of crystallinity of the blend, resulting in higher values than those predicted from extrapolation for the wholly amorphous blend. The latter infers a T_g of less than -30°C for pure PVF_2.

The *FT*i.r. evidence for the miscibility of PVF_2 and PVAc is more apparent when blend compositions containing no crystalline material are used. The study reveals that the interactions of PVAc and PMMA have the same impact on the spectrum of PVF_2 in the respective blends. Therefore it is concluded that the modes of dipole–dipole interactions in the PVF_2/PVAc and PVF_2/PMMA blends are the same.

The samples used in this study were hydrolysed to yield PVF_2/poly(vinyl alcohol) blends. Thermal and spectroscopic analyses of these blends will be reported in a subsequent paper[26].

REFERENCES

1 Bernstein, R. E., Paul, D. R. and Barlow, J. W. *Polym. Eng. Sci.* 1978, **18**, 683
2 Paul, D. R., Barlow, J. W., Bernstein, R. E. and Wahrmund, D. C. *Polym. Eng. Sci.* 1978, **18**, 1225
3 Belke, R. E. Thesis, State University of New York—College of Environmental Science and Forestry, Syracuse, 1985
4 Cabasso, I. *Am. Chem. Soc. Org. Coat. Plast. Chem.* 1979, **40**, 669
5 Jakabhazy, S. Z. and Zeman, L. J. US Patent 4302334, 1981
6 Mijovic, J., Luo, H. L. and Han, C. D. *Polym. Eng. Sci* 1982, **22**, 234
7 Morra, B. S. and Stein, R. S. *J. Polym. Sci., Polym., Phys. Edn.* 1982, **20**, 2243
8 Morra, B. S. and Stein, R. S. *J. Polym. Sci., Polym. Phys. Edn.* 1982, **20**, 2261
9 Imken, R. L., Paul, D. R. and Barlow, J. W. *Polym. Eng. Sci.* 1976, **16**, 593
10 Bernstein, R. E., Cruz, C. A., Paul, D. R. and Barlow, J. W. *Macromolecules* 1977, **10**, 681
11 Paul, D. R. and Altamirano, J. O. *Adv. Chem. Ser.* 1975, **142**, 371
12 Hourston, D. J. and Hughes, I. D. *Polymer* 1977, **18**, 1175
13 Krause, S. in 'Polymer Blends', (Eds D. R. Paul and S. Newman), Academic Press, New York, 1978, Vol. 1, Ch. 2
14 Coleman, M., Zarian, J., Varnell, D. F. and Painter, P. C. *J. Polym. Sci., Polym. Lett. Edn.* 1977, **15**, 745
15 Roerdink, E. and Challa, G. *Polymer* 1980, **21**, 1161
16 Leonard, C., Halary, J. L., Monnerie, L., Broussoux, D., Servet, B. and Micheron, F. *Polym. Commun.* 1983, **24**, 110
17 Hahn, B., Wendorff, J. and Yoon, D. *Macromolecules* 1985, **18**, 718
18 Prest, W. M. and Luca, D. J. *J. Appl. Phys.* 1975, **46**, 4163
19 Lovenger, A. J. in 'Developments in Crystalline Polymers', (Ed. D. C. Bassett), Applied Science, London, 1982, Vol. 1, Ch. 5
20 Boyer, R. F. *J. Macromol. Sci.–Phys. (B)* 1973, **8**(3–4), 503
21 Brandrup, J. and Immergut, E. H. (Eds) 'Polymer Handbook', Wiley-Interscience, New York, 1966
22 Kwei, T. K., Frisch, H. L., Radigan, W. and Vogel, S. *Macromolecules* 1977, **10**, 157
23 Wu, S. *J. Polym. Sci.* 1987, **25**, 557
24 Cortili, G. and Zerbi, G. *Spectrochim. Acta (A)* 1967, **23**, 285
25 Flory, P. J. and Yoon, D. Y. *Macromolecules* 1984, **17**, 862
26 Belke, R. and Cabasso, I. in preparation
27 Stokr, J. *et al. Coll. Czech. Chem. Commun.* 1963, **28**, 1946
28 Nakagawa, K. and Ishida, Y. *Kolloid Z. Z. Polym.* 1973, **251**, 103